ISSN 1027-4510, Journal of Surface Investigation: X-ray, Synchrotron and Neutron Techniques, 2016, Vol. 10, No. 5, pp. 1060–1066. © Pleiades Publishing, Ltd., 2016.
Original Russian Text © S.V. Filatov, M.Yu. Brazhnikov, A.A. Levchenko, A.M. Lihter, 2016, published in Poverkhnost', 2016, No. 10, pp. 69–76.

Turbulence in the System of Capillary Waves on the Surface of Water

S. V. Filatov[a, b], M. Yu. Brazhnikov[a, b], A. A. Levchenko[a, b, c, *], and A. M. Lihter[c]

[a] *Institute of Solid-State Physics, Russian Academy of Sciences, Chernogolovka, Moscow oblast, 142432 Russia*
[b] *Institute for Theoretical Physics, Russian Academy of Sciences, Chernogolovka, Moscow oblast, 142432 Russia*
[c] *Astrakhan State University, Astrakhan, 414056 Russia*
**e-mail: levch@issp.ac.ru*

Received February 9, 2016

Abstract—The experimental results of studying wave turbulence in a system of capillary waves on the surface of water in a cylindrical vessel are presented. Waves on the surface are excited by vertical vibrations of the water-filled vessel with accelerations below the parametric-instability threshold at a fixed frequency f_p or in the frequency band from 30 to 50 Hz. The deviation of the surface from equilibrium is recorded by a laser beam reflecting from water. It is shown experimentally that the position of the high-frequency boundary of the inertial range f_b of the turbulent cascade is shifted towards high frequencies with an increase in the pump amplitude A and described by the power function $f_b \sim A^\beta$ with index β equal to 1.2 ± 0.1 for monochromatic pumping and 1.10 ± 0.15 for broadband pumping. The value of the index β for monochromatic pumping is close to the theoretical estimate; for broadband pumping, it is less by a factor of 2.5. In the dissipation region $f > f_b$, the turbulent distribution is damped exponentially with the characteristic frequency f_d depending on the amplitude and spectral characteristic of the excitation force. It follows from the amplitude dependences that the frequency f_d is proportional to the frequency of the boundary of the inertial range f_b.

Keywords: capillary waves, wave turbulence, monochromatic and broadband pumping

DOI: 10.1134/S102745101605027X

INTRODUCTION

Turbulence in a system of waves, together with vortex turbulence, plays a significant part in many processes occurring on Earth and in the Universe. It is the subject of intensive studies in many systems: on the ocean surface, in the atmosphere, and in plasma [1]. Turbulence on the surface of water in the gravity-capillary frequency range has been studied by many investigators in recent decades [2–5]. The waves were excited via different techniques. For example, in [2], special paddles (wave makers) immersed into the liquid were used. However, in most works, waves are generated via parametric instability of the liquid surface which produces forced vertical vibrations with accelerations above a certain threshold value (Faraday instability) [3–5]. A distinctive feature of this technique is a high level of wave excitation immediately after the appearance of instability on the surface. This feature of the excitation technique does not allow one to work with small amplitude waves. In addition, as it turned out, strong excitation results not only in the nonlinear interaction of waves but also in the observed generation of vortex motion [6, 7]. Recently, it was shown in [8, 9] that vorticity is formed as a result of the interaction of nonlinear waves with nonparallel wave vectors, i.e., in the two-dimensional space of wave vectors $\mathbf{k}$. In [10], waves on the surface of a cylindrical cell were excited by a ring touching the water surface near the cell walls. Only the radial mode was excited on the surface. In this case, standing waves on the surface are described by a Bessel function with parameter Rk (R is the cell radius). The scalar k plays the part of the wave number: at large values of R/λ, ($\lambda = 2\pi/k$ is the length of the excited wave) and at a large distance $r \gg \lambda$ from the cell center in a narrow angular sector, a cylindrical wave can be considered as a plane wave with the wave number k in one-dimensional k-space. The experimental results [10] turned out to be in good agreement with the theory of weak (wave) turbulence [1].

This report presents experimental results on turbulence in a system of waves on the surface of water in the case where the waves are excited by vertical vibrations of the cell due to the boundary effect of wetting at accelerations below the threshold value for the appearance of the Faraday instability in a cylindrical cell, when vortex motion is not yet observed, and in a square cell, where vortex motion is well developed at these levels of pumping.

We recall that one can distinguish three frequency ranges in a turbulent cascade: the pump region in which the system is supplied with energy; the inertial range where the energy is transferred mainly due to nonlinear interaction; and the dissipation region in which the vibration energy dissipates as heat. In the inertial range, the pair correlation function of surface

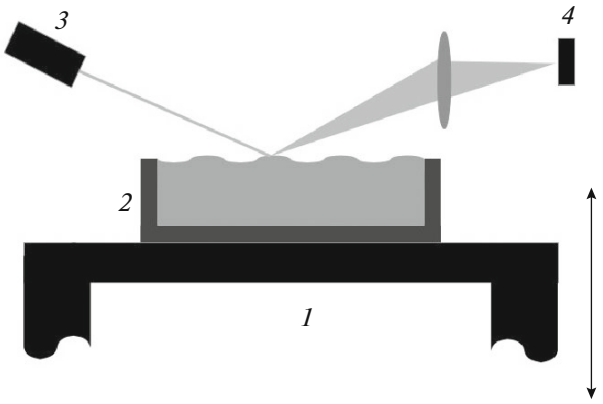

Fig. 1. Scheme of the experiment: (*1*) vibration platform; (*2*) water-filled vessel; (*3*) laser; and (*4*) photodetector.

deviations from equilibrium I_ω is described by a power function

$$I_\omega \sim \omega^m,$$

where $\omega = 2\pi f$ is the frequency and power index m depends on the spectral characteristic of the excitation force [1]: $m = -17/6$ for broadband pumping and $-23/6$ for narrowband pumping. The theoretical estimates for m were verified in experiments with liquid hydrogen [11] and water [2].

The boundary of the inertial range is defined as the characteristic frequency f_b at which the nonlinear time of interaction between waves becomes equal to the time of viscous damping [10]. The position of the frequency f_b depends both on the properties of the liquid surface and on the pump characteristics: amplitude and width of the excitation band. The theory predicts a power dependence for the position of the boundary of the inertial range ω_b on the pump amplitude A:

$$f_b \sim A^\beta. \quad (1)$$

The power index β depends on the pumping type: for monochromatic pumping, $\beta = 4/3$; for broadband pumping, 12/5 [11]. The boundary of the inertial range in a system of capillary waves was observed for the first time on the surface of liquid hydrogen [10].

The dissipation region can be characterized by two parameters: position of the boundary of the inertial range f_b and characteristic frequency of exponential damping f_d. At frequencies $f > f_b$, the power law of the distribution I_ω passes to exponential damping [11]

$$I_\omega \sim \exp(-f/f_d). \quad (2)$$

An exponential drop in the turbulent cascade at frequencies above f_b was observed in the system of capillary-gravity waves on the surface of liquid hydrogen and helium [12, 13]. In experiments with liquid hydrogen [12], it was shown in the case of broadband pumping that the characteristic frequency f_d increases with an increase in the excitation-force amplitude by the power law $f_d \sim A^{0.85}$.

The dimensions of the experimental cells are finite; therefore, the spectrum of surface excitations is of discrete character. This imposes additional restrictions on the fulfillment of energy and momentum conservation laws [14]. It was shown experimentally in [15, 16] that energy transfer to both high and low frequencies can be organized by choosing the cell dimensions in the process of pumping at some frequencies.

The aim of this work is to carry out comprehensive studies of the high-frequency boundary of the inertial range f_b and characteristic frequency f_d as functions of the excitation-force amplitude on the surface of water in cylindrical and square cells when the pump amplitudes are less than the threshold value at which the parametric Faraday instability occurs.

EXPERIMENTAL

The experimental setup schematically shown in Fig. 1 consists of a vibration platform *1*, a water-filled experimental cell *2* mounted onto it, and vibration detection systems *3* and *4*.

The experimental cells had the form of a beaker with a diameter from 65 to 130 mm and depth of 10 mm, as well as the form of a rectangle with sides of 49 × 50 mm and a depth of 10 mm. Water is poured above the brim of the beaker to form a concave meniscus. During vertical oscillations of the cell, the equilibrium radius of the meniscus varies depending on the cell acceleration, which excites oscillations of the water surface. Waves on the water surface were excited by supplying an oscillating electric voltage from a digital generator to the input of the vibration platform. The following kinds of pumping were used: monochromatic pumping at the resonance frequency, narrowband pumping with a band width of about 1 Hz, and broadband pumping of 30–50 Hz. By the pump amplitude A in the case of monochromatic excitation, we mean the amplitude of the electric signal fed to the vibration platform. In the case of narrowband or broadband pumping, the root-mean-square value of the electric signal fed to the vibration platform is taken as the amplitude A. We note that the elevation of the fundamental harmonic wave on the surface of the water is directly proportional to the amplitude A (acceleration of the cell in the vertical direction) during monochromatic pumping.

Oscillations of the water surface were recorded using a system described earlier in [17]. A laser beam at a small grazing angle is incident on the water surface and is reflected from it. The reflected laser beam power depends on the angle of reflection. Therefore, the presence of waves on the surface leads to temporal variations in the power of the reflected beam $P(t)$. The reflected beam is focused on the photodetector, the electrical signal from which is digitized and recorded into the computer memory.

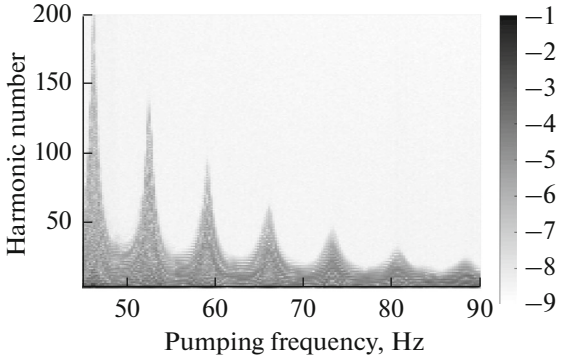

Fig. 2. Frequency and amplitude distributions of waves on the surface of water in a 65-mm-diameter cylindrical cell. On the right, the scale of amplitudes is presented in arbitrary units.

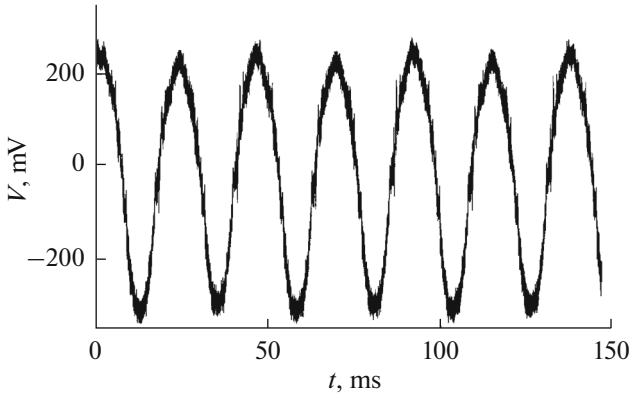

Fig. 3. Record of the signal from the photodetector when the water surface is excited by monochromatic pumping at a frequency of 46 Hz in the 65-mm-diameter cell.

Waves on the water surface are detected in the "wide beam" mode, i.e., the characteristic wavelength on the water surface is much less than the size of the laser-beam spot. In this mode, the power detected by the photodetector is an integral characteristic of the surface shape. As was shown in [17], if the light power is uniformly distributed over the laser spot on the liquid surface, the pair correlation function I_ω is directly proportional to the squared Fourier component P_ω^2 of the reflected-laser-beam power:

$$I_\omega \sim P_\omega^2.$$

Figure 2 shows the experimental frequency distribution of wave amplitudes upon the excitation of waves in a cell with a diameter of 65 mm and depth of 10 mm by a monochromatic force at a fixed pump frequency f_p. The pump frequency increases from 46 to 90 Hz with a step of 0.1 Hz. On the abscissa axis, the frequency is plotted in Hz; on the ordinate axis, the number of the detected harmonic N with the frequency Nf_p.

The estimate shows that, in the frequency range from 45 to 90 Hz, the distance between resonance peaks exceeds the peak width, the viscous broadening of resonance peaks is $2\nu\omega^{4/3}(\rho/\sigma)^{2/3}$ (ρ is the density, ν is the kinematic viscosity, and σ is the surface tension coefficient of water), i.e., the spectrum of surface vibrations in this frequency range is discrete.

Figure 3 presents an example of a recorded signal detected by the photodetector during the monochromatic excitation of waves at a frequency of 46 Hz in a cylindrical cell. We note that the main variations in the power of the reflected laser beam are caused by oscillations of the water surface at the pump frequency.

EXPERIMENTAL RESULTS

Figure 4 presents the spectrum P_ω^2 obtained by the Fourier transform of the signal shown in Fig. 3. Let us note the features in this distribution. The largest peak positioned to the left on the frequency scale corresponds to the frequency of the excitation monochromatic force $f_b = 46$ Hz. The arrow in the spectrum marks the boundary of the inertial range f_b. At frequencies above f_b, there is a dissipation region where the turbulent energy flux rapidly attenuates. In the range between the pump region and the boundary of the inertial range, there are peaks corresponding to resonances that appear as a result of the three-wave interaction with frequencies multiple to f_b. It is seen that the peak maxima in the spectrum within the inertial range well fit a straight line which corresponds to the power law of the distribution with a power index close to −3.

With increasing excitation-force amplitude, the position of the high-frequency boundary of the inertial range f_b is shifted towards high frequencies. The frequency f_b is determined by the compensated spectra P_ω^2/ω^γ. The power index γ is selected such that the spectrum P_ω^2/ω^γ does not depend on frequency in the inertial range. The value f_b is determined as the frequency at which the deviation from the plane spectrum P_ω^2/ω^γ amounts to 50%.

HIGH-FREQUENCY BOUNDARY OF THE INERTIAL RANGE f_b

Analysis of the dependences $f_b(A)$ shows that the power index β depends on the excitation-force amplitude. Figure 5 present the frequency and amplitude distributions of waves during two sequential cycles of an increase and decrease in the excitation-force amplitude at a pump frequency equal to $f_p = 44$ Hz. The boundary of the inertial range is located between the grey and black colors and increases with increasing pumping amplitude. It is well seen in the figure that the frequency of the high-frequency boundary of the inertial range at small pump amplitudes grows according to a law which is somewhat stronger than the linear

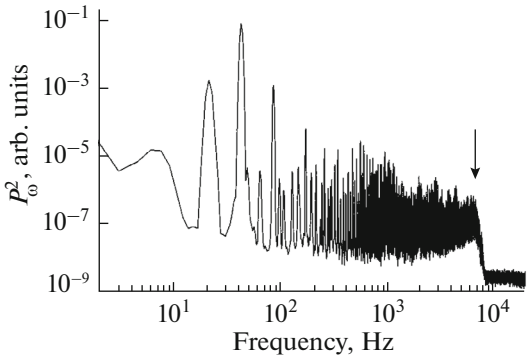

Fig. 4. Turbulent cascade on the water surface in the 65-mm-diameter cell. Monochromatic pumping at a frequency of 46 Hz.

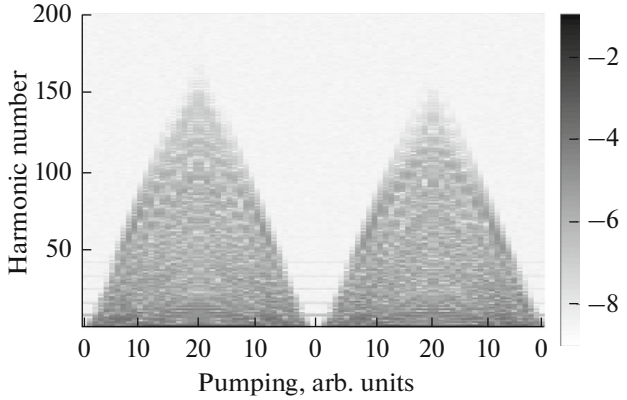

Fig. 5. Frequency and oscillation amplitude distributions of waves during two sequential cycles of increasing and decreasing amplitude of the excitation force at a frequency f_p = 44 Hz. The excitation-force amplitude is shown in arbitrary units. The diameter of the cell is 65 mm.

one, i.e., $\beta > 1$ up to the 80th harmonic of the pump frequency. At high pump amplitudes, the power index β approaches unity.

Figure 6 presents the frequency of the boundary of the inertial range f_b as a function of the monochromatic pumping amplitude on the logarithmic scale. The dependences were obtained in 65- and 130-mm-diameter cylindrical cells at pump frequencies of 45.5 and 44 Hz, respectively. It is seen that the obtained points of f_b in the plots in logarithmic coordinates well fit a straight line, which corresponds to the power dependence of the boundary frequency of the inertial range on the pump amplitude $f_b \sim A^\beta$. The experimental values of the power index β lie within the range from 1.3 ± 0.2 for all cylindrical cells. We note that the theoretical value of β for monochromatic pumping is equal to 4/3 [13]. Thus, one can conclude that the experimental values well agree with the theoretical estimate.

When passing from monochromatic pumping to broadband pumping, good power dependences $f_b \sim A^\beta$ are also observed in a wide range of excitation-force amplitudes but the power index β is less than in the case of monochromatic pumping.

Figure 7 presents the frequencies of the boundary of the inertial range as a function of the broadband-pumping amplitude on the logarithmic scale for two cells. It is seen that the experimental points are well described by power functions of the amplitude. The power index β varies from 1.32 in the 65-mm-diameter cell to 1.14 in the 130-mm-diameter cell; on the average, $\beta = 1.23 \pm 0.09$.

As in the case of monochromatic pumping, experimental points in the plots well fit a straight line, which corresponds to a power dependence of the boundary frequency of the inertial range on the pump amplitude. We note that the obtained values of the power index β are on average 1.10 ± 0.15 and considerably differ from the theoretical value equal to 12/5 [11].

To be sure that the obtained power dependences $f_b(A)$ are not a feature of waves in a cylindrical cell, the experiments were replicated on an almost square cell with sides of 49 × 50 mm. Figure 8 presents the frequencies of the high-frequency boundary of the inertial range f_b as functions of the monochromatic and broadband excitation-force amplitude. It is seen that the dependence $f_b(A)$ also can be described by a power function with a power index equal to 0.95 ± 0.03. It turned out that the presence of vortices on the surface had no significant effect on wave turbulence.

We note that the boundary of the inertial range is weakly expressed in the obtained spectra P_ω^2 in the case of narrowband pumping (the bandwidth is ~1 Hz). As a consequence, the dependence of the boundary of the inertial range on the pumping amplitude was not identified.

CHARACTERISTIC FREQUENCY OF DAMPING f_d

As was mentioned above, the turbulent cascade at frequencies exceeding f_b is damped due to viscous losses. Figure 9 presents the characteristic frequency f_d as a function of the monochromatic pumping amplitude in double logarithmic coordinates for two cells. We note that the frequency f_d in the 65-mm-diameter cell (Fig. 9a) increases by a power law as the excitation-force amplitude increases to the value $A = 12$. At the same, in the cell with a larger diameter, a steady increase in the characteristic frequency is observed with an increase in the pumping level. Approximation of the experimental data by the power dependence $f_d \sim A^\alpha$ yields the following values of the power index: $\alpha = 1.18$ for the 65-mm-diameter cell for the growth portion and $\alpha = 1.38$ for the 130-mm-diameter cell; on average, $\alpha = 1.28 \pm 0.10$.

Figure 10 shows the distribution P_ω^2 in semilogarithmic coordinates during broadband pumping in the

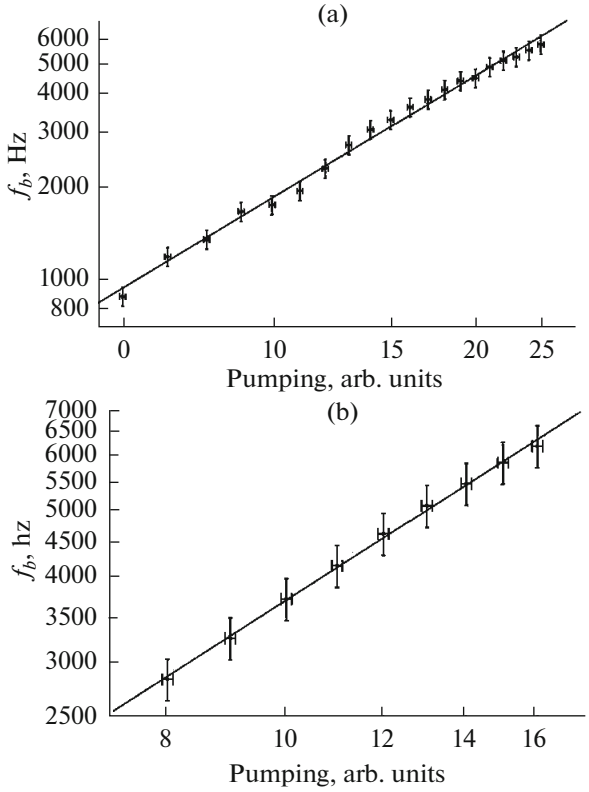

Fig. 6. High-frequency boundary of the inertial range as a function of the monochromatic-pumping amplitude in cylindrical cells with diameters of (a) 65 mm, f_p = 45.5 Hz, and (b) 130 mm, f_p = 44.0 Hz.

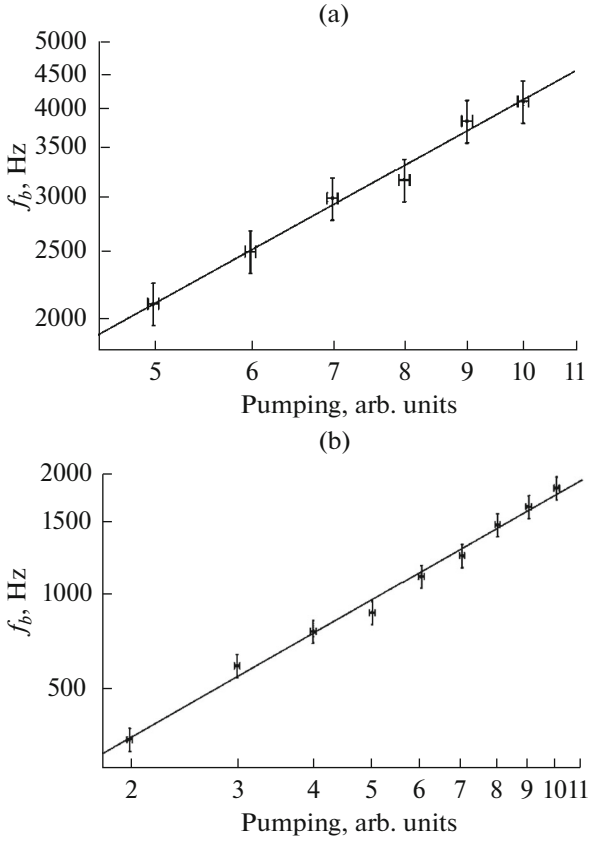

Fig. 7. High-frequency boundary of the inertial range f_b as a function of the broadband-pumping amplitude in the range of 30–50 Hz in cylindrical cells with diameters of (a) 65 and (b) 130 mm.

range of 30–50 Hz. The distribution was obtained in the 65-mm-diameter cell. The pump amplitudes in arbitrary units amount to 3 : 7 : 10. The arrows in each spectrum show the position of the boundary of the inertial range f_b at 650, 2500, and 4300 Hz, respectively. At frequencies above f_b, exponential damping is observed in the dissipation region. For clarity, straight lines drawn in the figure emphasize the exponential dependences P_ω^2. The characteristic frequencies calculated by dependences (2) for the distributions shown in Fig. 8 are 430, 1050, and 1550 Hz, respectively.

In the case of broadband pumping, the dependence of the frequency f_d on the pumping amplitude is steady. Figure 11 presents the dependences of f_d on the broadband-pumping amplitude on the logarithmic scale in two cells. It is seen that points of the plot well fit a straight line corresponding to a power dependence on the amplitude with a power index close to values obtained by dependences of the boundary frequency of the inertial range on the pump amplitude. The obtained values of α are close to 1.1.

DISCUSSION

Experimental data testify that the amplitude dependences of the frequency of the high-frequency boundary of the inertial range f_b can be well described by power functions of the amplitude A^β. The power index in the case of monochromatic pumping amounts on average to $\beta = 1.23 \pm 0.09$, which is close to the theoretical estimate $\beta = 4/3$. The amplitude dependence of the characteristic frequency for exponential damping of the turbulent cascade is described by a power function with an index $\alpha = 1.28 \pm 0.10$. Therefore, it can be confirmed that the frequency f_b in the case of monochromatic pumping is directly proportional to f_d, $f_b = mf_d$. The value of the proportionality factor is 4–5, i.e., the characteristic frequency f_d is less by several times than the boundary frequency of the inertial range.

In the case of broadband pumping, the power indices are on average equal to $\beta = 1.10 \pm 0.15$ and $\alpha = 1.12 \pm 0.03$, i.e., they almost coincide. Therefore, one can assume that $f_b = nf_d$ and n is equal to 3–4. This means that harmonics from the dissipation region, in both the cases of monochromatic pumping and broadband excitation, interact mainly with modes positioned within the inertial range [12] but below the frequency of its boundary. It is difficult to find how close these modes are to the boundary of the inertial range; how-

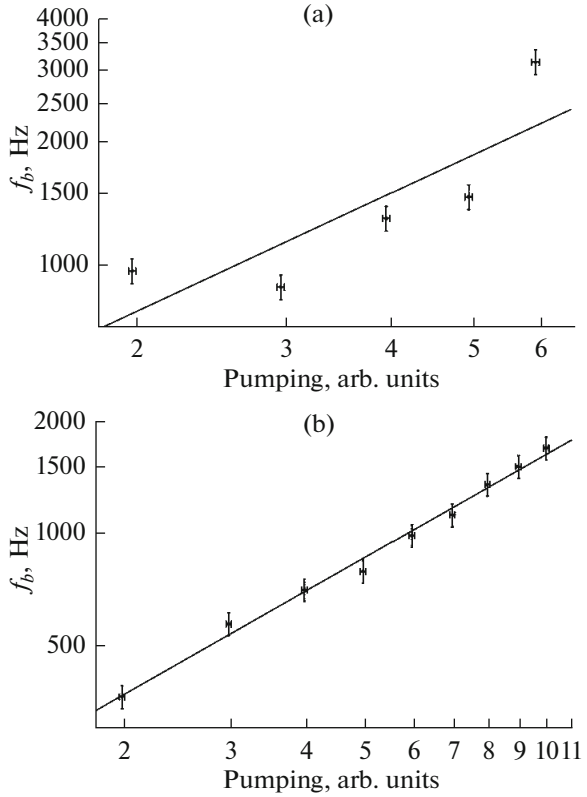

Fig. 8. Frequency of the high-frequency boundary of the inertial range f_b as a function of the (a) monochromatic- and (b) broadband-pumping amplitude in a cell with dimensions of 49 × 50 mm.

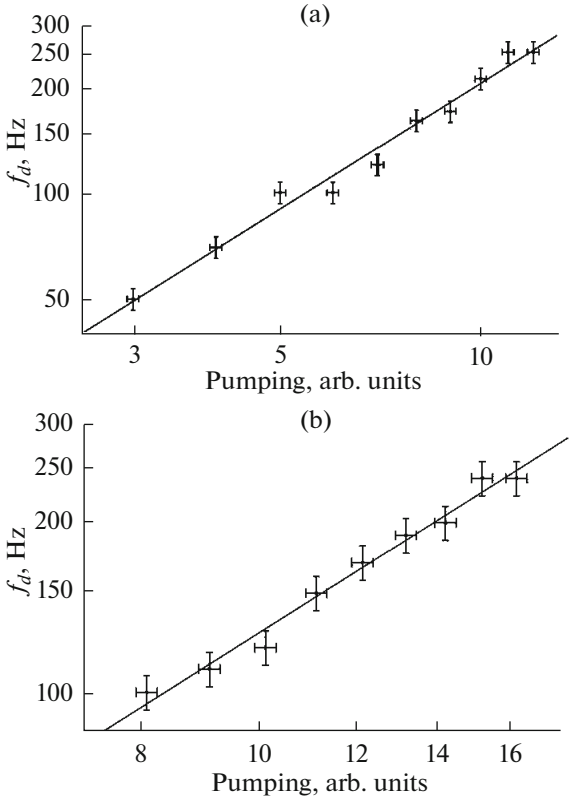

Fig. 9. Characteristic frequency f_d as a function of the excitation-force amplitude during monochromatic pumping (a) at a frequency of 45.5 Hz in a 65-mm-diameter cell and (b) at a frequency of 44.0 Hz in a 130-mm-diameter cell.

ever, they are considerably higher than the pumping frequency f_p.

We note that the characteristic frequency f_d in experiments with superfluid helium in the case of monochromatic pumping was close to the pump frequency f_p [13] and less than the boundary frequency of the inertial range by tens of times. At the same time, in experiments with liquid hydrogen in the case of broadband pumping, the characteristic frequency f_d was only a few times lower than the frequency of the high-frequency boundary of the inertial range f_b and considerably exceeded the pumping frequency f_p [12].

Thus, one can assume that the ratio of frequencies f_b, f_p, and f_d in experiments on the surface of water, in both cases of broadband and monochromatic pumping and in experiments with broadband pumping of the surface of hydrogen, are qualitatively close. In all these cases, waves from the dissipation region interact mainly with modes from the inertial range, far from the pump region and boundary of the inertial range.

Let us pay attention to the fact that, at high levels of monochromatic pumping, the frequency f_b increases with an increase in amplitude by a law which is weaker than the linear law (Fig. 5). The discrepancy in the value of the power index β obtained in the experiment and estimated from the theory in the case of the broadband excitation of waves remains unclear. We note that this discrepancy is observed in experiments both with waves on the water surface with different techniques of surface excitation [18] and on the surface of liquid hydrogen [10] and superfluid helium [13]. In all those

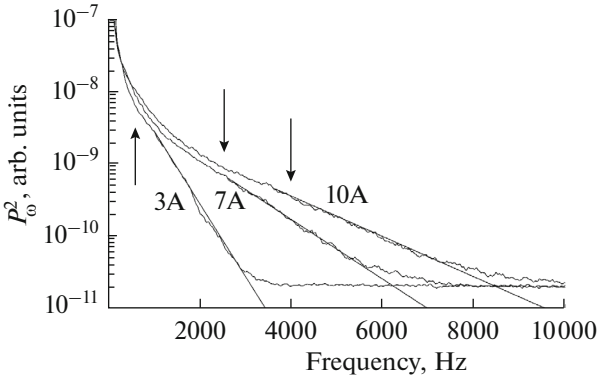

Fig. 10. Turbulent distributions on the surface of water in a 65-mm-diameter cell upon pumping in the range of 30–50 Hz. The pump amplitudes are shown in arb units near the curves.

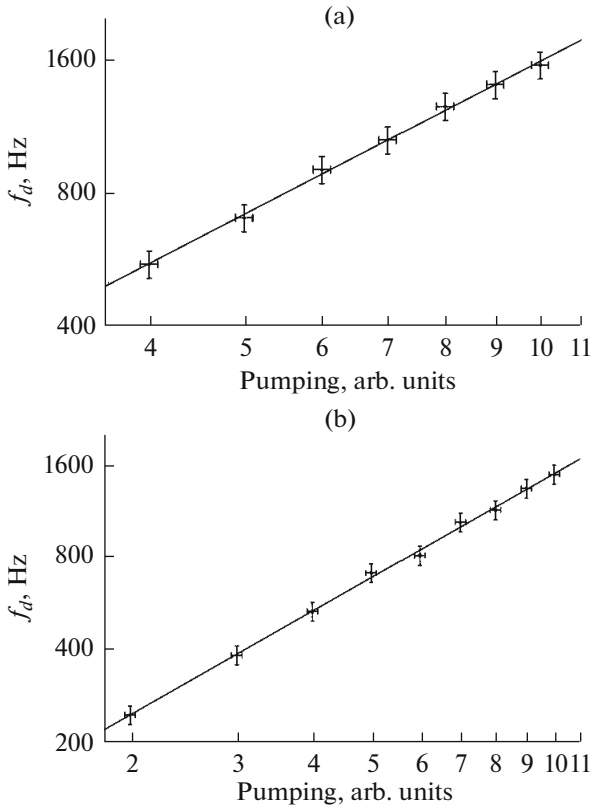

Fig. 11. Characteristic frequency f_d as a function of the excitation-force amplitude upon broadband pumping at frequencies from 30 to 50 Hz in a cell with a diameter of (a) 65 and (b) 130 mm.

experiments, the angular amplitudes of the waves at the pump frequency are of the same order, which is related to features of the technique for detecting the deviation of a liquid's surface from the equilibrium position [17], and the kinematic viscosity of the liquids changes by approximately 100 times. This means that discrepancies in the values of β are not related to the properties of the liquids but are determined by other causes. To clarify this problem, additional investigations are required.

CONCLUSIONS

In this work, it has been shown experimentally that if the turbulent state on the water surface is excited by monochromatic or broadband pumping, the high-frequency boundary of the inertial range and characteristic frequency in the dissipation region differ by several times and qualitatively similarly increase with increasing pump amplitude by a power law with a power index close to the theoretically estimated value for monochromatic excitation. In the case of broadband pumping, a considerable discrepancy between the experimental and theoretically estimated values of index β is observed.

ACKNOWLEDGMENTS

We are grateful to A.V. Lokhov for help in preparing the experiments. This work was supported by the Russian Science Foundation, project no. 14-22-00259.

REFERENCES

1. V. E. Zakharov, V. S. L'vov, and G. Falkovich, *Kolmogorov Spectra of Turbulence I* (Springer, 1992).
2. E. Falcon, C. Laroche, and S. Fauve, Phys. Rev. Lett. **98**, 094503 (2007).
3. E. Henry and M. T. Levinsen, Europhys. Lett. **52** (1), 27 (2000).
4. M. Shats, H. Punzmann, and H. Xia, Phys. Rev. Lett. **104**, 104503 (2010).
5. P. Denissenko, S. Lukaschuk, and S. Nazarenko, Phys. Rev. Lett. **99**, 014501 (2007).
6. M. G. Shats, H. Xia, and H. Punzmann, Phys. Rev. E: Stat., Nonlinear, Soft Matter Phys. **71**, 046409 (2005).
7. A. Von Kameke, F. Huhn, G. Fernandez-Garcia, A. P. Munuzuri, and V. Perez-Munuzuri, Phys. Rev. Lett. **107**, 074502 (2011).
8. S. V. Filatov, M. Yu. Brazhnikov, and A. A. Levchenko, JETP Lett. **102** (7), 432 (2015).
9. S. V. Filatov, V. M. Parfenyev, S. S. Vergeles, M. Yu. Brazhnikov, A. A. Levchenko, and V. V. Lebedev, Phys. Rev. Lett. **116**, 054501 (2016).
10. M. Yu. Brazhnikov, G. V. Kolmakov, and A. A. Levchenko, JETP **95**, 447 (2002).
11. I. V. Ryzhenkova and G. E. Falkovich, Sov. Phys. JETP **98**, 1931 (1990).
12. M. Yu. Brazhnikov, L. V. Abdurakhimov, S. V. Filatov, and A. A. Levchenko, JETP Lett. **93**, 31 (2011).
13. M. Yu. Brazhnikov, A. A. Levchenko, I. A. Remizov, and S. V. Filatov, JETP Lett. **95**, 751 (2012).
14. E. A. Kartashova, Phys. D (Amsterdam, Neth.) **54**, 125 (1991).
15. M. Yu. Brazhnikov, A. A. Levchenko, L. P. Mezhov-Deglin, and I. A. Remizov, JETP Lett. **100**, 669 (2014).
16. L. V. Abdurakhimov, M. Yu. Brazhnikov, A. A. Levchenko, A. M. Likhter, I. A. Remizov, Fiz. Nizk. Temp. (Kiev) **41** (3), 215 (2015).
17. M. Yu. Brazhnikov, A. A. Levchenko, and L. P. Mezhov-Deglin, Prib. Tekh. Eksp., No. 6, 31 (2002).
18. M. Yu. Brazhnikov, G. V. Kolmakov, A. A. Levchenko, and L. P. Mezhov-Deglin, Europhys. Lett. **58**, 510 (2002).

Translated by A. Nikol'skii